# Supplementary Information

## Surface Structure-Regulated Cell Membrane Penetration by Monolayer Protected Nanoparticles

Ayush Verma[1], Oktay Uzun[1], Yuhua Hu[2], Ying Hu[1], Hee-Sun Han[3], Nicky Watson[4], Suelin Chen[1], Darrell J. Irvine[1,5*] & Francesco Stellacci[1*]

[1]*Department of Materials Science and Engineering, MIT, Massachusetts 02139, USA*

[2] *Department of Chemical Engineering, MIT, Massachusetts 02139, USA*

[3]*Department of Chemistry, MIT, Massachusetts 02139, USA*

[4]*Department of Biology, MIT, Massachusetts 02139, USA*

[5]*Department of Biological Engineering, MIT, Massachusetts 02139, USA*

## 1. Supplementary Figures:

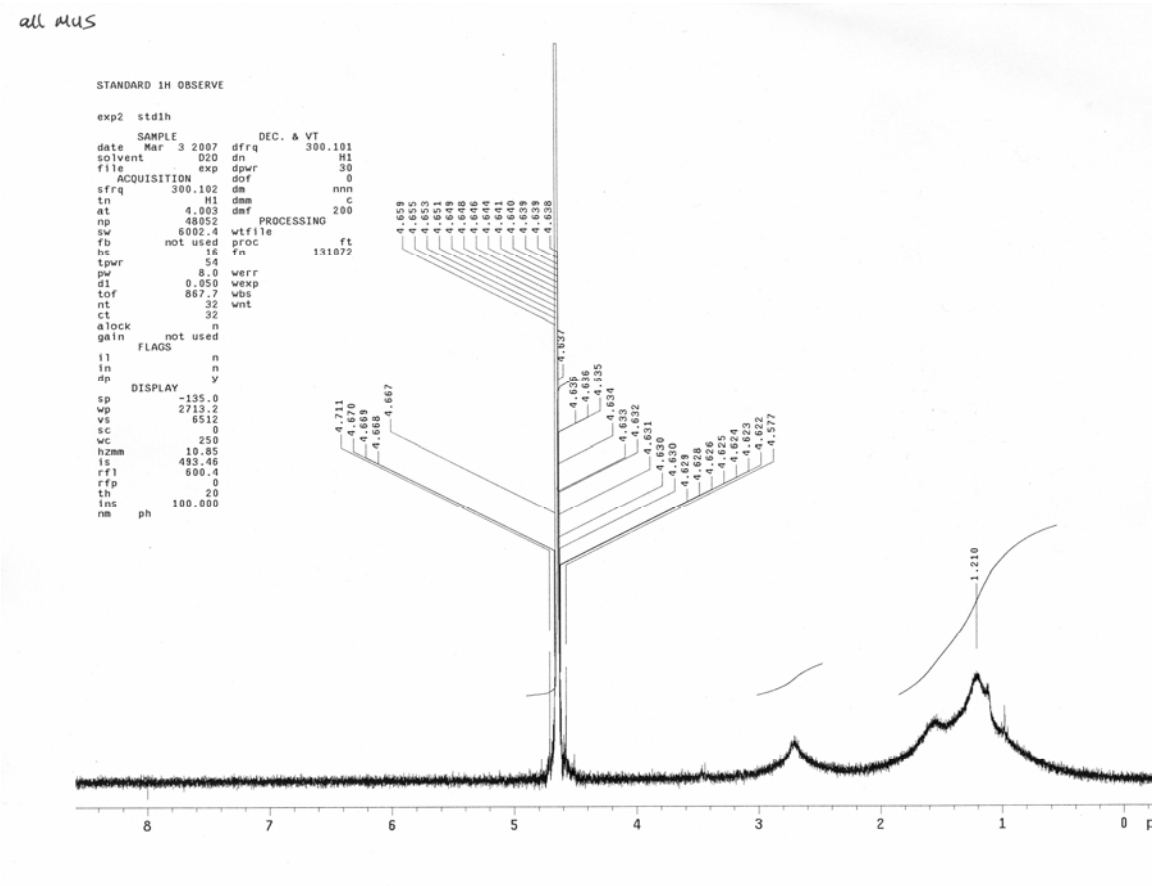


**Supplementary Figure 1.** NMR spectrum of the MUS particles taken in $D_2O$.

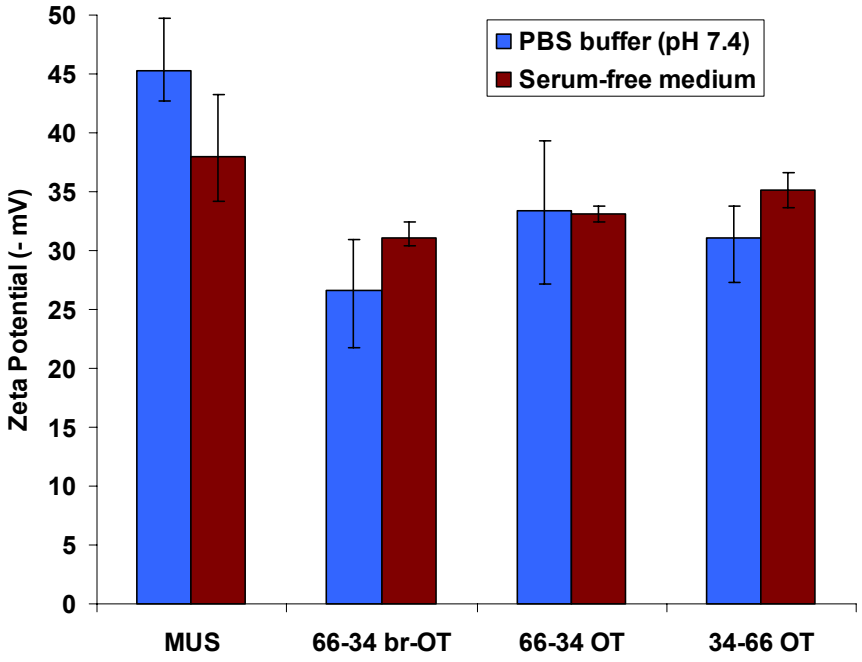


**Supplementary Figure 2.** Zeta potential of the nanoparticles measured both in PBS buffer (pH 7.4) (10mM Sodium phosphate and 140 mM NaCl) and serum-free RPMI 1640 medium.

**Supplementary Table 1.** Diameter of nanoparticles before and after incubation with serum-containing media measured by TEM and DLS

| | TEM total diameter[a] before incubation (nm) | TEM total diameter[a] after incubation (nm) | DLS diameter before incubation (nm) | DLS diameter after incubation (nm) |
|---|---|---|---|---|
| MUS | 7.4±1.3 | 7.5±0.9 | 6.8±0.2 | 12.0±0.4 |
| 66-34 br-OT | 7.4±1.2 | 7.6±1.0 | 8.0±0.2 | 10.0±0.4 |
| 66-34 OT | 7.6±1.0 | 7.4±0.8 | 7.2±0.2 | 7.8±0.2 |

[a]Calculated by adding the metal core radii measured from TEM images and two times the MUS ligand length (3.1 nm) estimated using ChemBio3D Ultra 11.0 (Cambridgesoft)

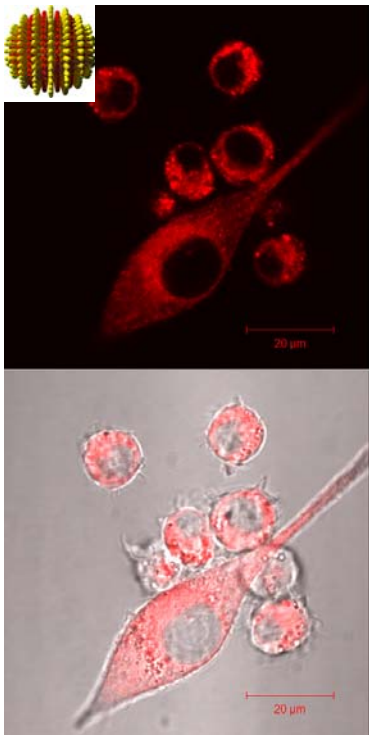


**Supplementary Figure 3.** Representative confocal image of DCs incubated with 34-66 OT nanoparticles in serum-free condition at 37°C.

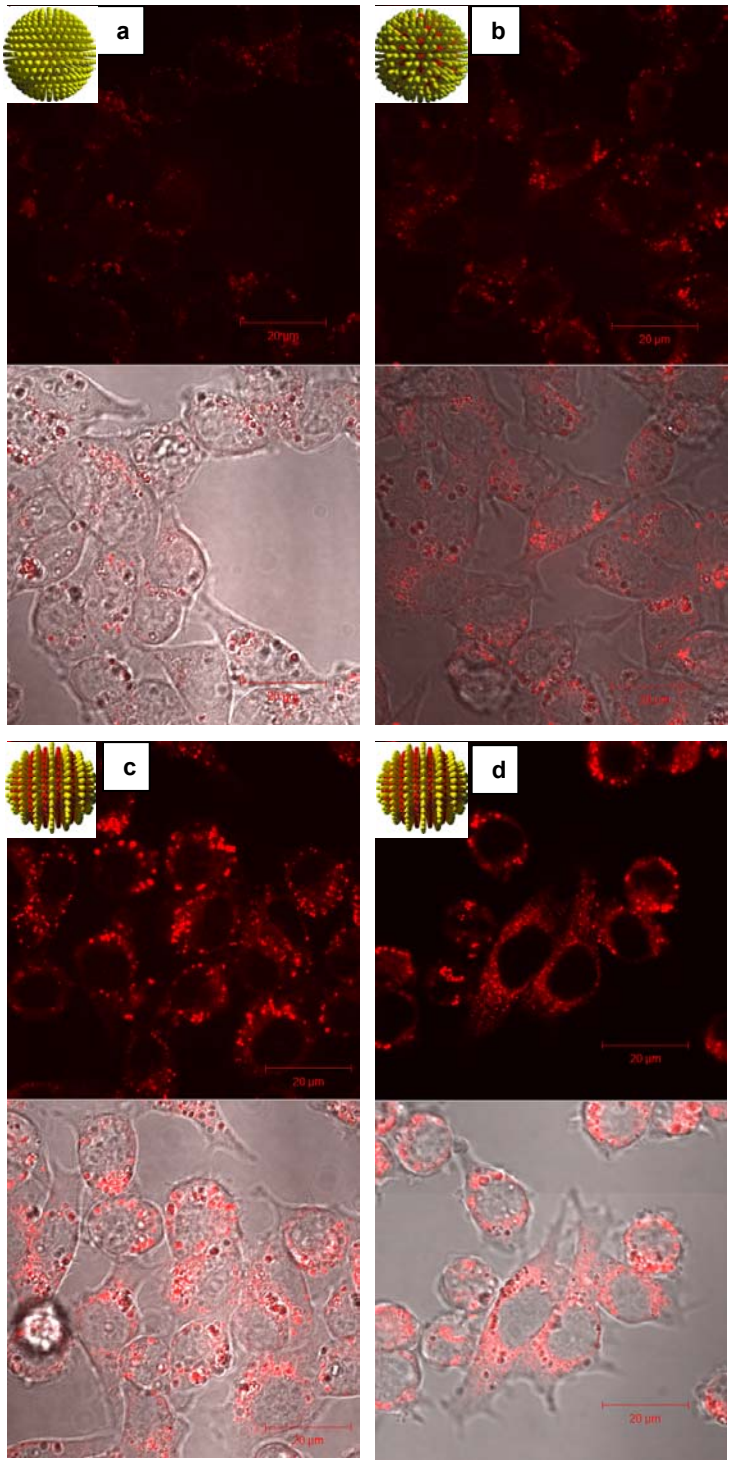


**Supplementary Figure 4.** Confocal images of DCs incubated with (a) MUS, (b) 66-34 br-OT, (c) 66-34 OT and (d) 34-66 OT nanoparticles in serum-containing medium (10% FBS) at 37ºC.

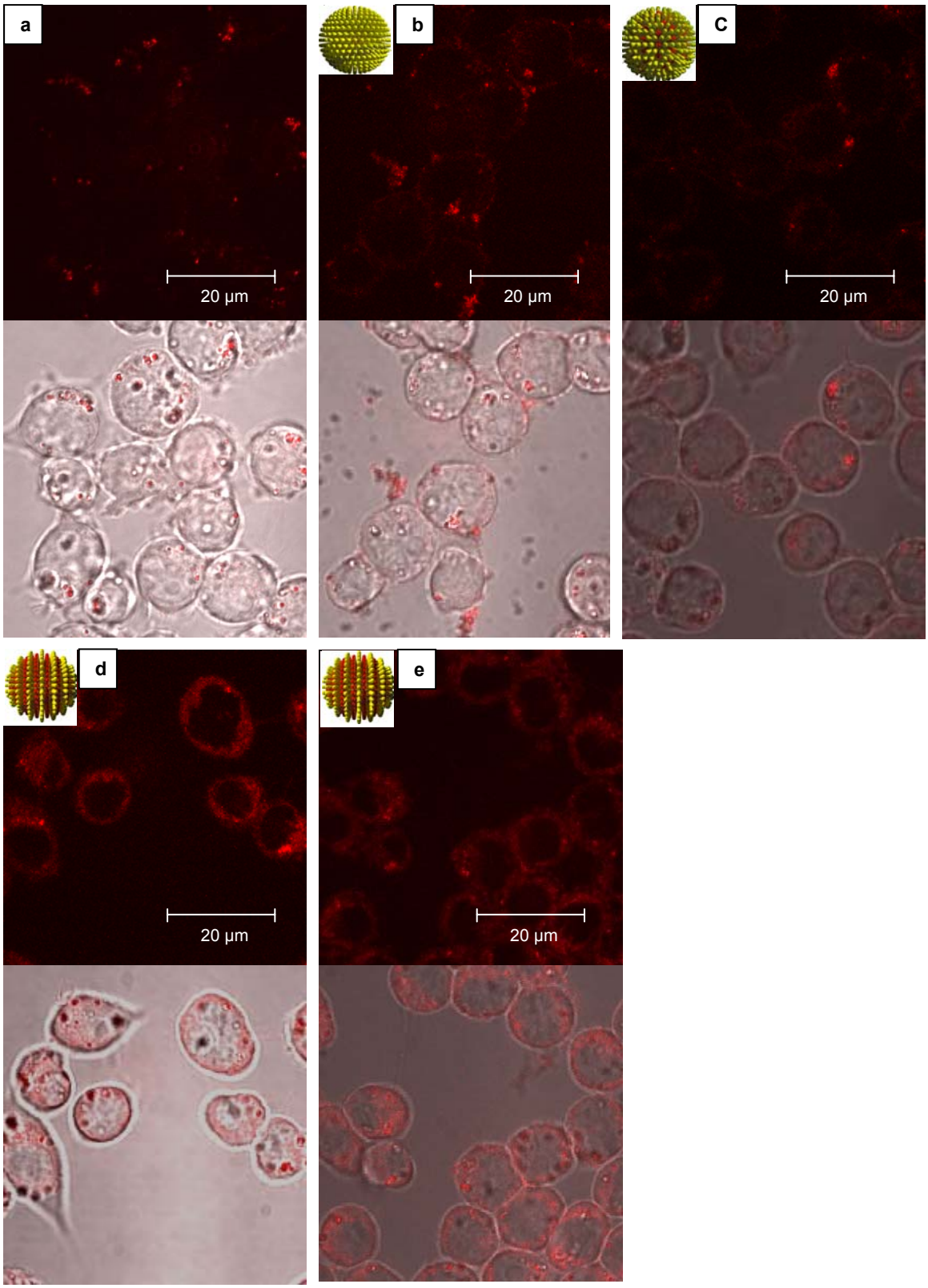
a
20 μm
b
20 μm
C
20 μm
d
20 μm
e
20 μm

**Supplementary Figure 5.** Confocal images of DCs incubated with nanoparticles in serum-free conditions at 4 ºC. Autofluorescence level of (a) untreated cells are similar to cells incubated with (b) MUS and (c) 66-34 br-OT. (d) 66-34 OT and (e) 34-66 OT nanoparticles display a much higher uptake.

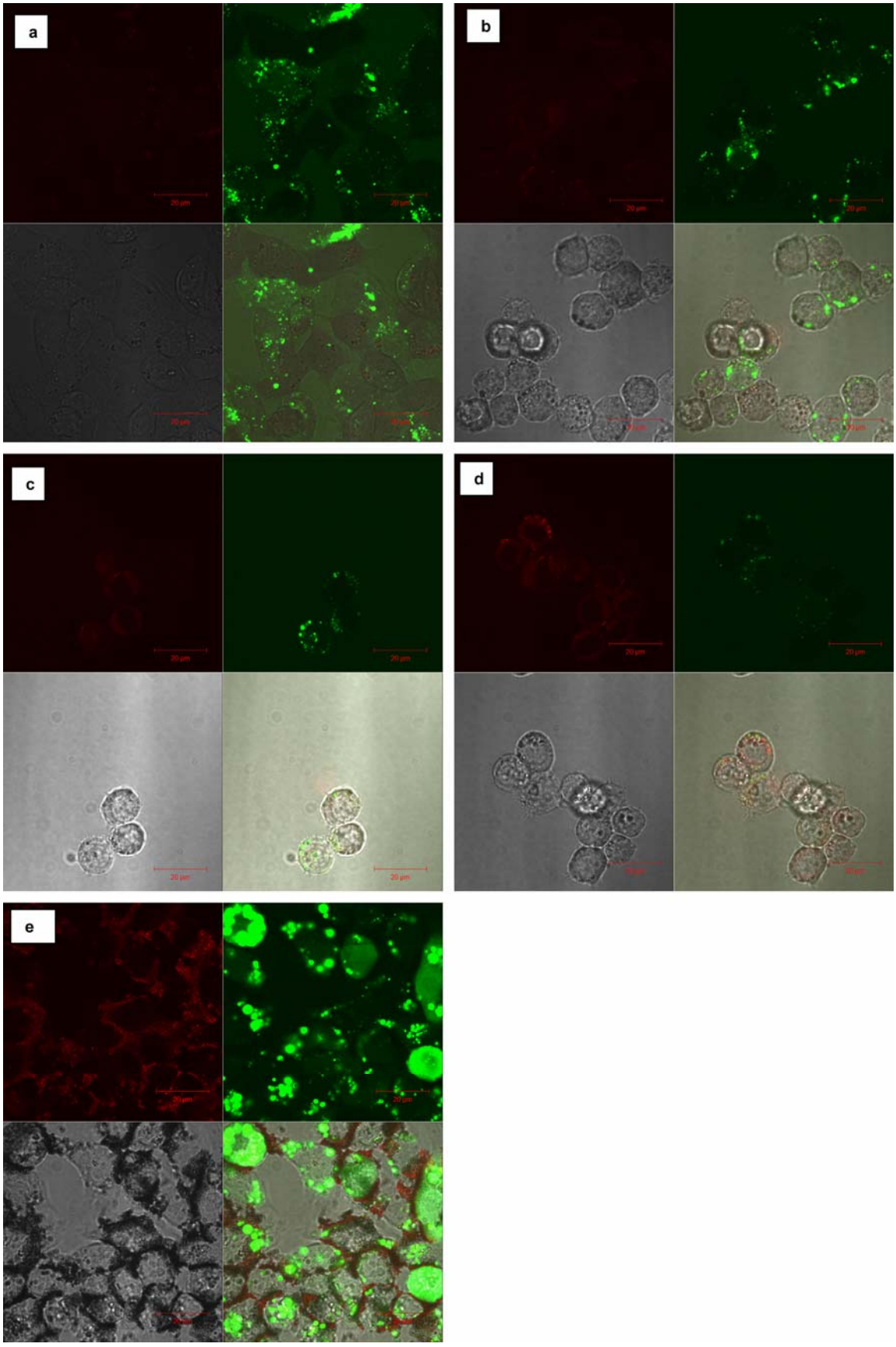
a
b
c
d
e

**Supplementary Figure 6.** Confocal images of DCs incubated with Calcein (a) alone, and in the presence of fluorescently labeled (b) MUS, (c) 66-34 br-OT, (d) 66-34 OT, and (e) TMA.

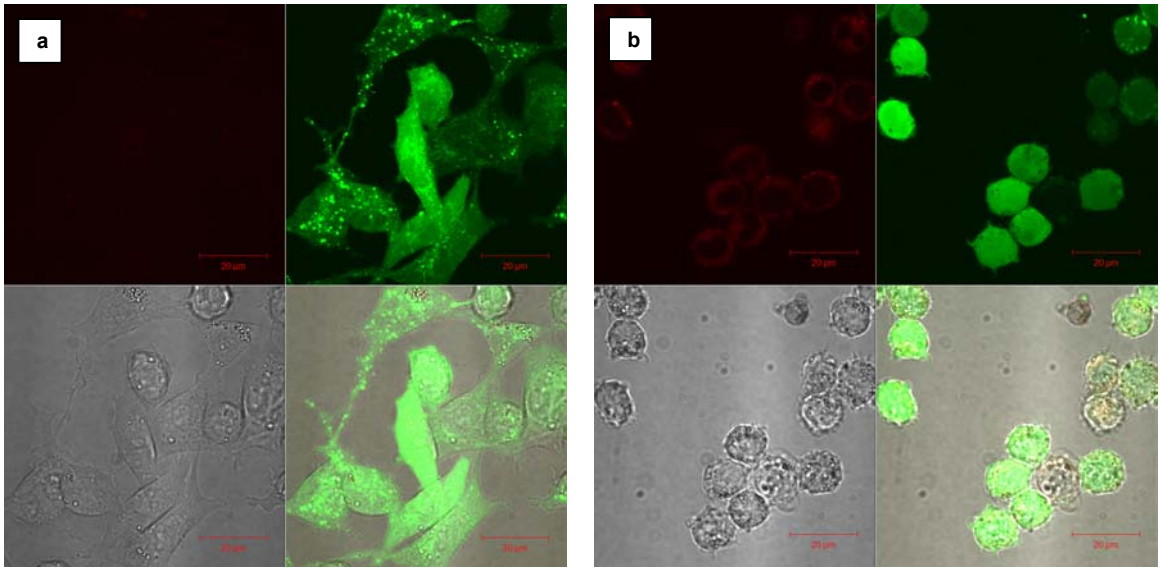


**Supplementary Figure 7.** Confocal images of DCs incubated with Calcein AM (a) alone, and in the presence of fluorescently labeled (b) 66-34 OT nanoparticles.

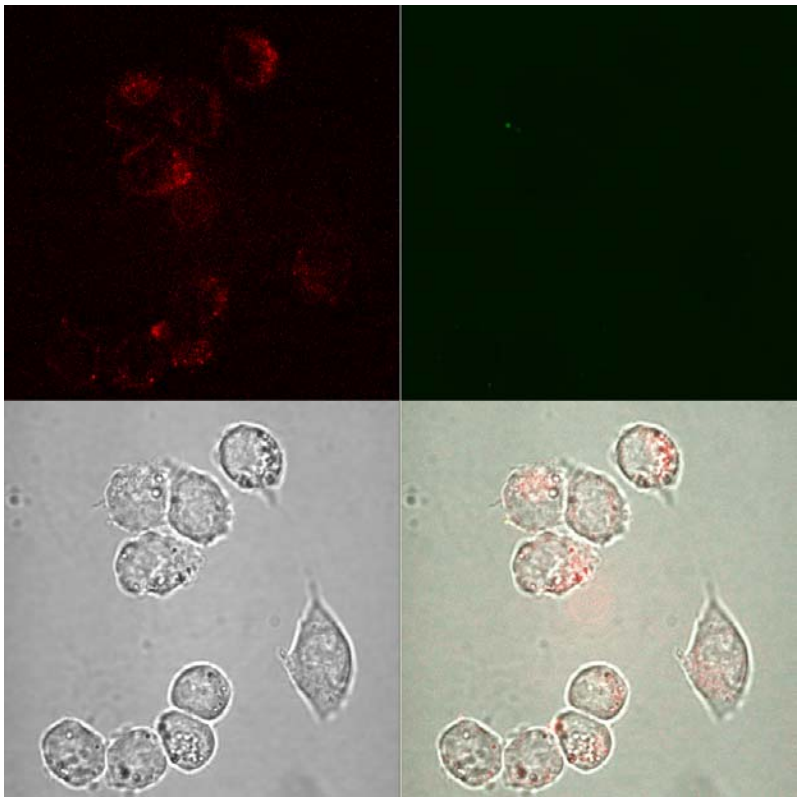

**Supplementary Figure 8.** Confocal images of DCs incubated for 5 min at 37°C in serum-free medium with calcein and 66-34 OT nanoparticles in the presence of sodium azide and 2-deoxyglucose to block active internalization.

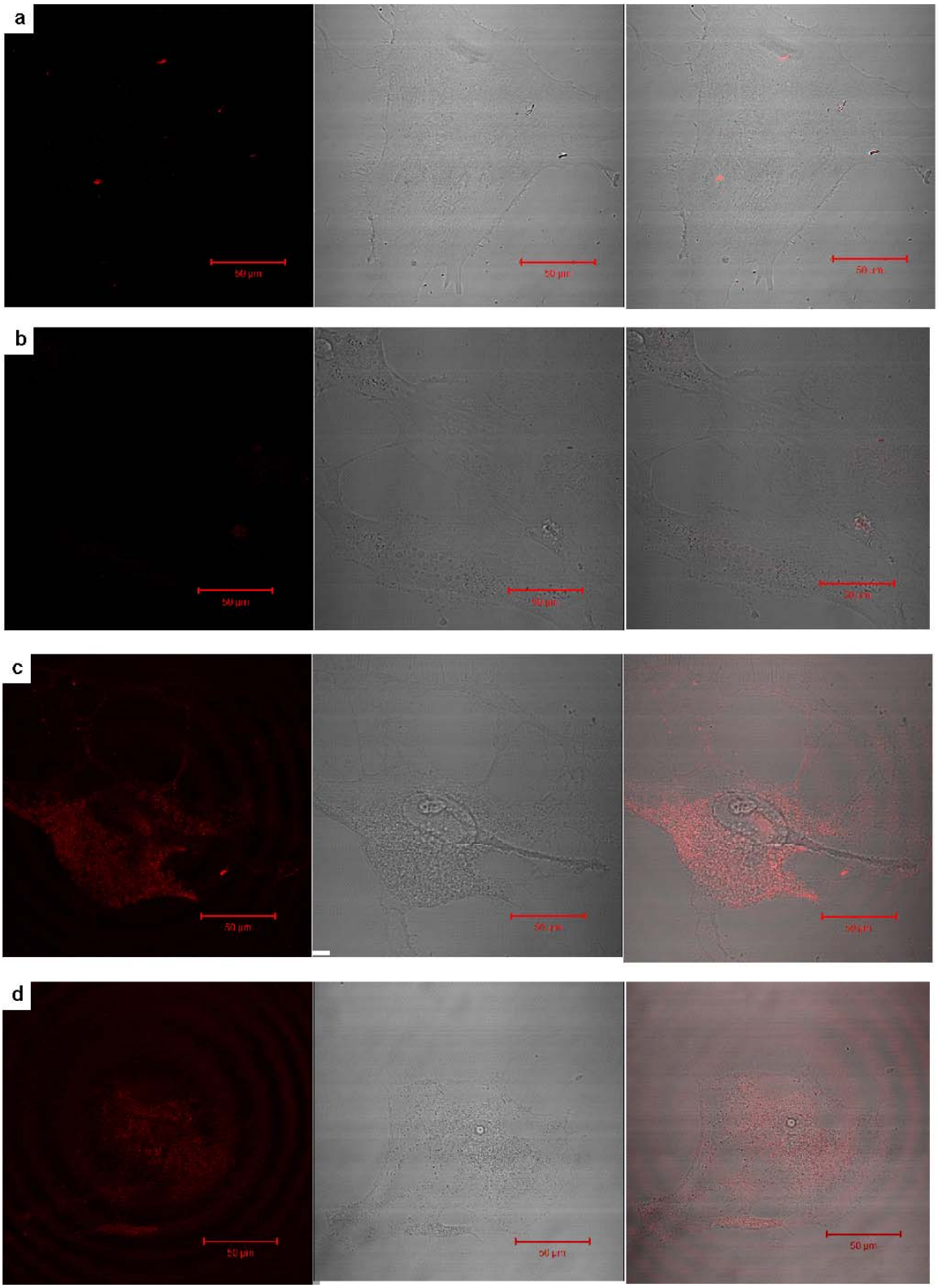
a
50 µm
50 µm
50 µm
b
50 µm
50 µm
50 µm
c
50 µm
50 µm
50 µm
d
50 µm
50 µm
50 µm

**Supplementary Figure 9.** Confocal images of MEFs incubated with nanoparticles in serum-free conditions at 4 ºC for 3 h. No nanoparticle uptake is seen with (a) MUS and (b) 66-34 br-OT, while (c) 66-34 OT and (d) 34-66 OT nanoparticles display cytosolic entry.

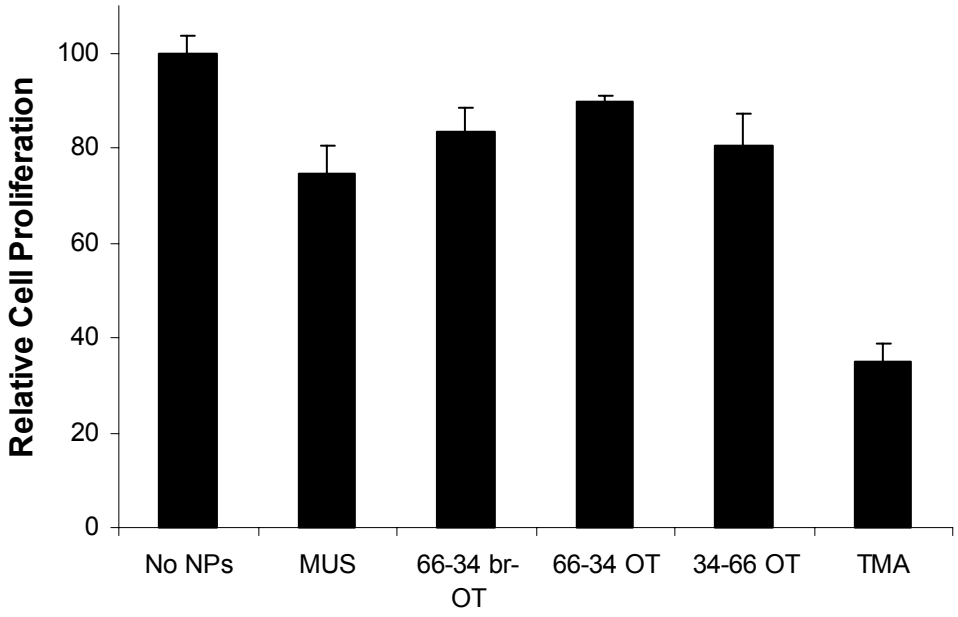


**Supplementary Figure 10.** Relative cell proliferation obtained through Cyquant NF assay after a 24-hour growth period of DCs. An ANOVA test on shows ($\alpha$=0.05) no statistically significant difference between relative proliferation percentages of all the sulfonate particles.

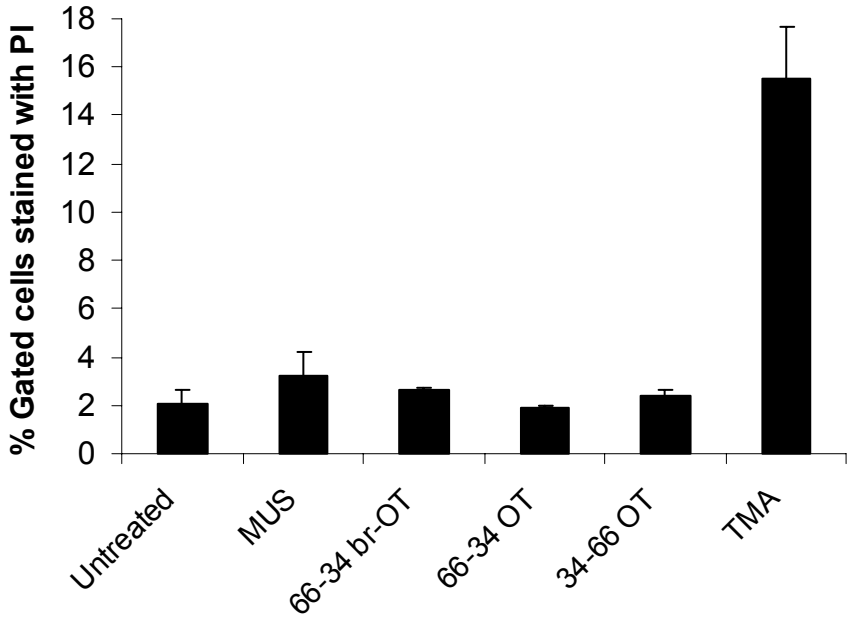


**Supplementary Figure 11.** Percentage of DCs stained with propidium iodide after 3 h incubation with nanoparticles in serum-free medium.

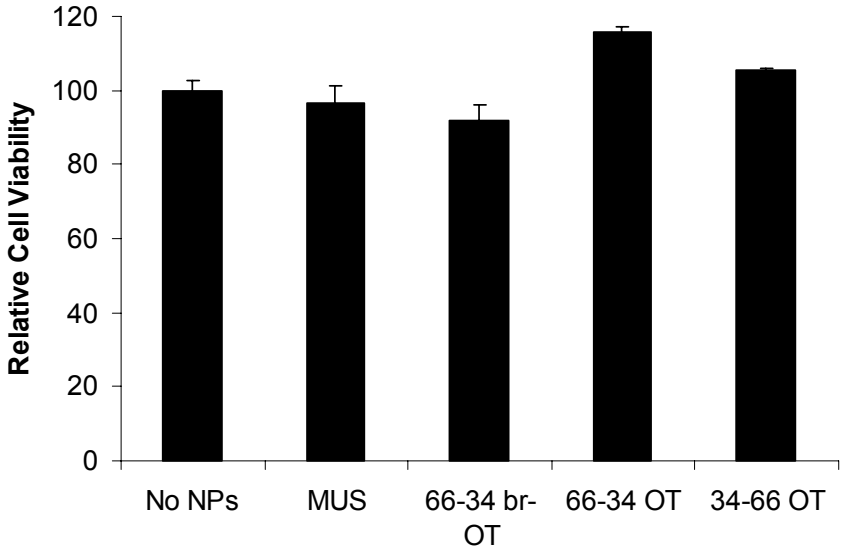


**Supplementary Figure 12.** Relative cellular viability of DCs obtained with MTT assay after 4 hours post nanoparticle incubation and washing. TMA particles were excluded in this study as their aggregates interfered with the absorbance reading at 570 nm.

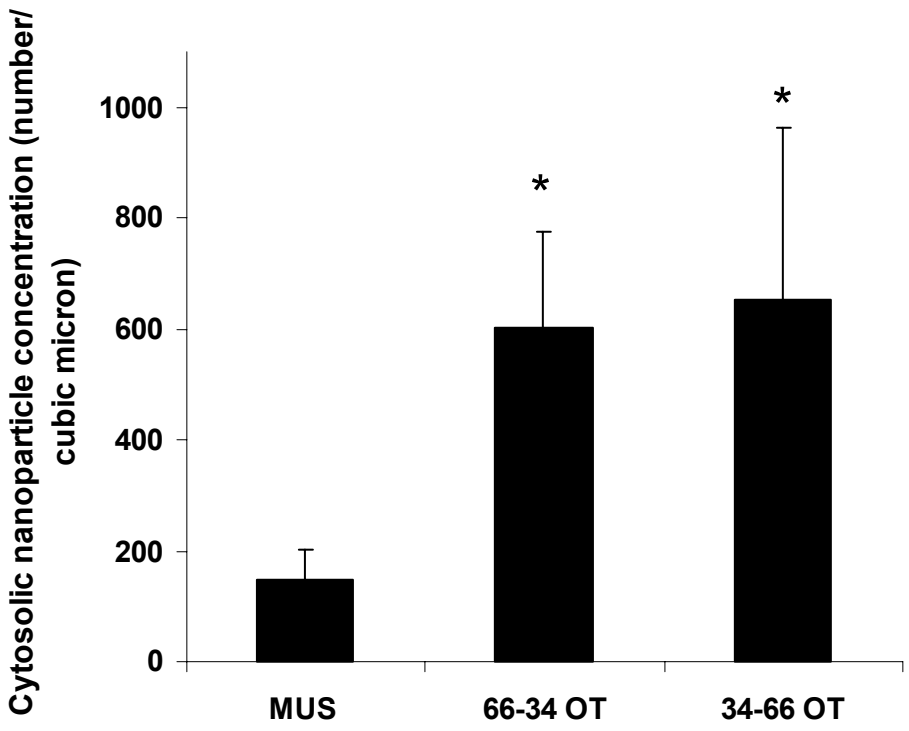


**Supplementary Figure 13.** Number of cytosolic nanoparticles per $\mu m^3$ (±st. dev.) in serum-containing condition, determined by scoring the localization of > 6000 particles per condition in DCs. *Statistically different from MUS ($P < 0.05$).

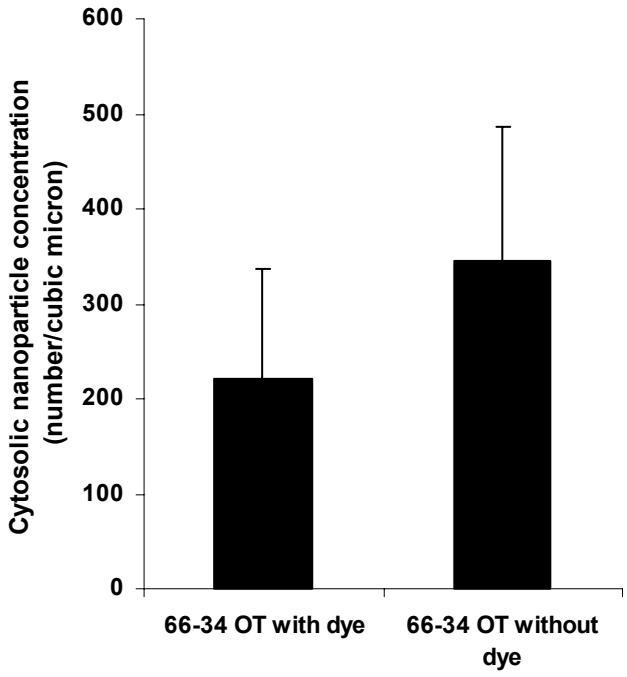


**Supplementary Figure 14.** Number of cytosolic nanoparticles per $\mu m^3$ (±st. dev.) in DCs for 66-34 OT particle with and without dye functionalization in serum-free condition after a 3 h incubation. Statistical analysis shows no difference ($P= 0.31$, $\alpha=0.05$, $n=3$).

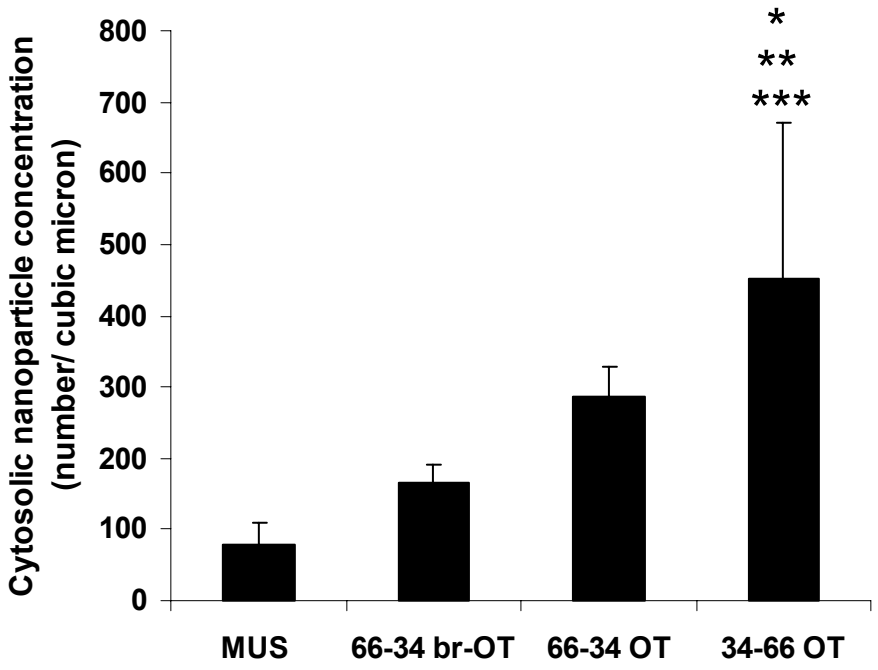


**Supplementary Figure 15.** Number of cytosolic nanoparticles per $\mu m^3$ (±st. dev.) in DCs in serum-free condition, determined by scoring the localization of > 6500 particles per condition. Statistical comparison of 34-66 OT shows a difference with MUS (*P < 0.05), with 66-34 br-OT (**P=0.08) and no difference with 66-34 OT (***P=0.23).

## 2. Supplementary Methods:

All chemicals were purchased from Sigma-Aldrich unless otherwise noted (all solvents were reagent grade), and were used as received. $^1$H-NMR spectra were acquired using a Varian Mercury-300. Unit mass determination was done using a Bruker Omniflex MALDI-TOF spectrometer. IR spectra of the nanoparticles were obtained on a Nicolet Nexus FTIR spectrometer. Optical spectra were acquired with an Agilent 8453 diode

array spectrophotometer. Nanoparticle core sizes were analyzed by Transmission Electron Microscopy (TEM) on a JEOL 200CX, at 200 kV. Zeta potentials (ζ) were measured using a Brookhaven ZetaPALS instrument. Thermogravimetric analysis (TGA) was performed by TA Instruments, TGA Q50. STM images were obtained using a Digital Instruments Multimode Nanoscope IIIa equipped with an E scanner installed in an acoustic chamber mounted on a vibration damping system. Cell sections for TEM were cut on a Reichert Ultracut E microtome with a Diatome diamond knife at a thickness setting of 50 nm. The sections were examined using a Jeol 1200EXM at 60 kV, a Phillips EM410 at 80kV or a FEI Tecnai spirit at 80kV.

## 2.1 Synthesis of Ligand Molecules

### 2.1.1 Synthesis of sodium 11-mercaptoundecanesulfonate

***Scheme 1:*** *Synthetic route for the synthesis of sodium 11-mercaptoundecanesulfonate*

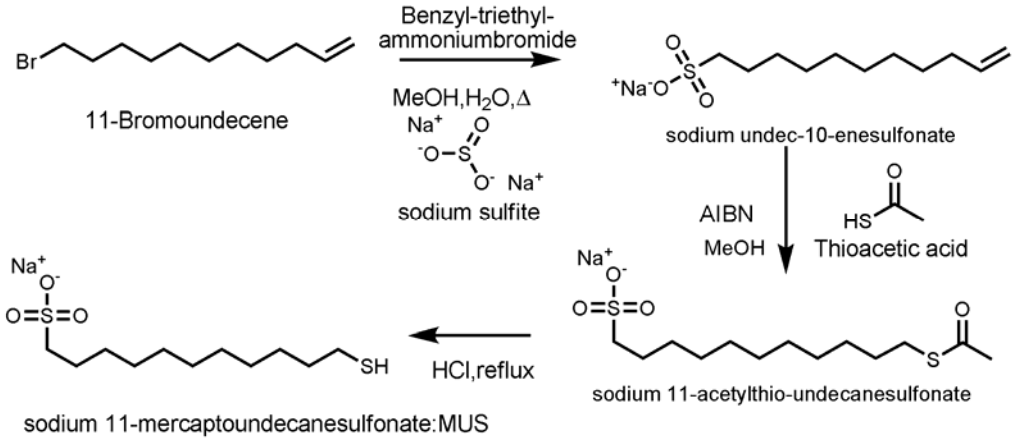

**Sodium undec-10-enesulfonate[46]:** 11-Bromoundecene (1.23 g, 5 mmol), sodium sulfite $Na_2SO_3$ (1.26 g, 10 mmol), benzyltriethyl-ammonium bromide (13.6 mg), MeOH (8 mL), and $H_2O$ (18 mL) were refluxed for 15 h. The mixture was extracted with ether (2 x 20 mL). The crystals, precipitated on cooling the aqueous solution to 0 $^0$C, were filtered and dried to give 0.9 g white solid (80%). $^1$H NMR ($D_2O$): 5.76 (m, 1H), 4.78 (m, 2H), 2.69 (t, 2H), 1.85 (q, 2H), 1.53 (m, 2H), 1.11 (br s, 12H).

**Sodium 11-acetylthio-undecanesulfonate:** The terminal alkene group was converted into thiol functionality with a modified literature synthesis[47]. Sodium undec-10-enesulfonate (0.9 g, 10 mmol) and thioacetic acid (2 mL, 26 mmol), azobisisobutylonitrile (AIBN, catalytic amt, 10 mg) in methanol (20 mL) were refluxed for 6 h. The volatiles were removed *in vacuo* and the residue was washed several times with ether, filtered and dried to give 0.8 g white solid. $^1$HNMR ($D_2O$): 2.69 (m, 4H), 2.17 (s, 3H), 1.53 (m, 2H), 1.39 (m, 2H), 1.11 (br s, 14H).

**11-mercaptoundecanesulfonate acid:** Sodium 11-acetylthio undecanesulfonate was refluxed in 10% HCl (20 mL) for 2 h. After removal of the solvents *in vacuo*, the solid was crystallized from $H_2O$, white solid (0.7g, 79%).$^1$HNMR ($D_2O$): 2.69 (t, 2H), 2.34 (t, 2H), 1.53 (m, 2H), 1.39 (m, 2H), 1.11 (br s, 14H). (Mass spectrum (ESI) found: m/z = 291.1068 calcd:291.1059)

2.1.2 Synthesis of 3,7 dimethyloctane 1-thiol

***Scheme 2:*** *Synthetic route for the synthesis of sodium 3,7-dimethyloctane-1-thiol*

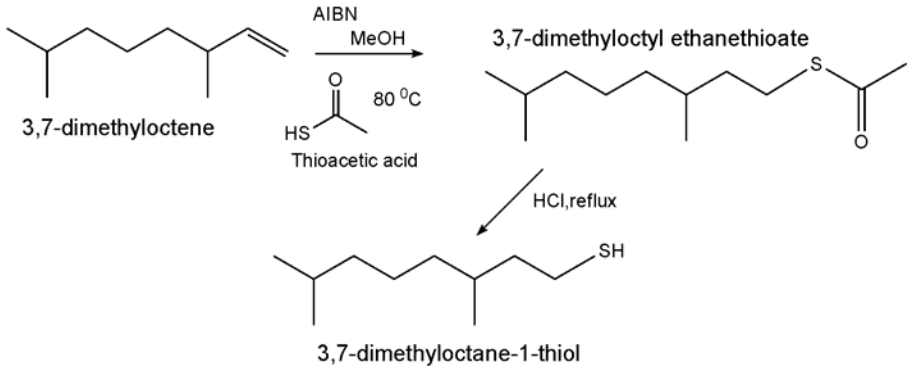


**3,7-dimethyloctyl ethanethiolate**: 3,7-dimethyl octene (1.4 g, 10 mmol), thioacetic acid (2 mL, 26 mmol), and AIBN (catalytic amt, 30 mg) in methanol (20 mL) were refluxed for 6 h. The volatiles were removed *in vacuo* to recover a yellow liquid (1.1 g, 79%).

**3,7-dimethyloctane thiol**: The terminal alkene group was converted into thiol functionality with a modified literature synthesis[47]. 3,7 dimethyloctyl ethanethiolate (1.1 g, 5 mmol) was refluxed in 10% HCl (20 mL) for 2 h. After removal of the acid *in vacuo*, the product was isolated (0.7 g, 0.70%). $^{1}$HNMR ($CDCl_3$): 2.6 (m, 2H), 1.5 (m, 4H), 1.3 (m, 2H), 1.1 (m, 4H), 0.87 (d, 3H), 0.85 (d, 6H) (Mass spectrum (ESI) found: m/z = 174.1445 calcd:174.1437)

2.1.3 Synthesis of BODIPY-SH

***Scheme 3:*** *Synthetic route for the synthesis of BODIPY-SH*

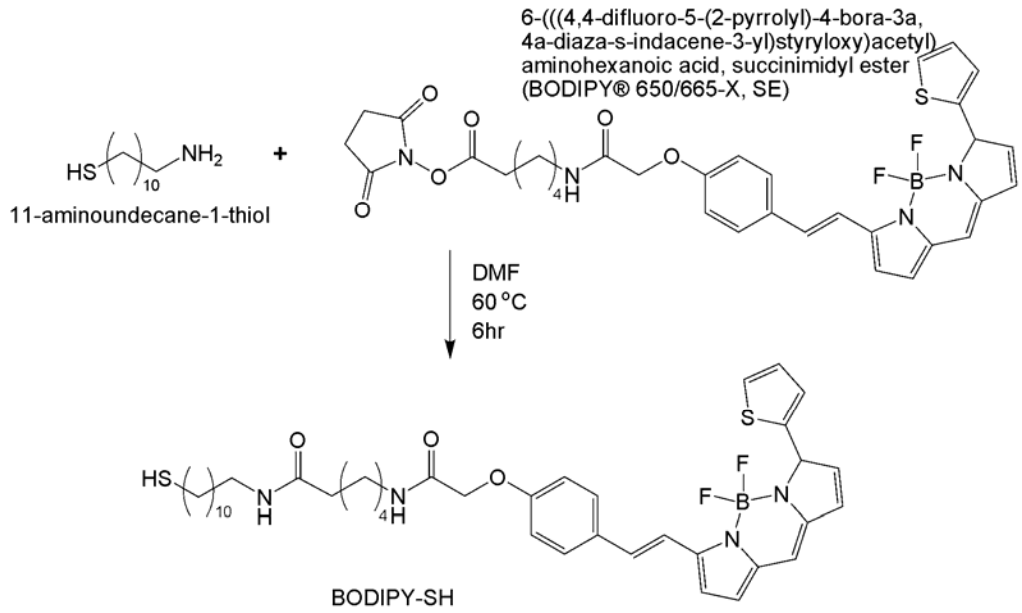


11-aminoundecane-1-thiol purchased from Prochimia (Poland) (0.93 mg, 4.6 μmol) was reacted with 6-(((4,4-difluoro-5-(2-pyrrolyl)-4-bora-3a,4a-diaza-s-indacene 3yl)styryloxy)acetyl) aminohexanoic acid, succinimidyl ester (BODIPY® 650/665-X, SE) purchased from Invitrogen (California, USA), (2.7 mg, 4.2 μmol) in 1 mL of DMF at $60^0$C for 6 h under inert atmosphere.

## 2.2 Synthesis of Nanoparticles

### 2.2.1 Synthesis of sulfonate nanoparticles

0.9 mmol of gold salt ($HAuCl_4$) was dissolved in 200 mL ethanol and 0.9 mmol of the desired thiol ligand mixture was added while stirring the reaction solution, then a saturated ethanol solution of sodium borohydride ($NaBH_4$) was added dropwise for 2 h. The solution was stirred for 3 h and the reaction vessel was then placed in a refrigerator overnight; precipitated particles were collected via vacuum filtration with quantitative filter paper. The residue was washed with ethanol, methanol and acetone and dried under vacuum. To completely remove unbound ligands, particles were dialysed using 5 inch segments of cellulose ester dialysis membrane (Pierce, SnakeSkin, MWCO 3500) that were placed in 1 L beakers of MilliQ water and stirred slowly. The beakers were recharged with fresh water ca. every 8 h over the course of 72 h. The NP solutions were collected from the dialysis tubes, and the solvent was removed under vacuum at < 45°C.

### 2.2.2 Synthesis of 11-mercaptoundecane-tetramethylammonium chloride (TMA) nanoparticles

TMA ligand was synthesized via previously reported procedures[47]. TMA-functionalized nanoparticles were synthesized using the same procedure described above for sulfonate nanoparticles.

2.2.3 Synthesis of fluorescently labeled nanoparticles

3.7 mg of BODIPY-SH dye was dissolved in 1.5 mL of a deionized water/ dimethylformamide mixture (2:1 vol:vol). This solution was used as a stock solution for all of the place exchange reactions. A typical reaction was performed as follows: 10 mg of ligand-coated nanoparticles (~$10^{-8}$ moles for 4.5 nm particles) were dissolved in 0.75 mL of DI water. Then, 75 μL (8 x $10^{-7}$ moles) of the dye stock solution was added to this nanoparticle solution and left stirring for 4 days in a sealed and dark environment according to known place exchange reaction procedures[48]. 5 drops (~ 0.1 mL) of the nanoparticle solution was placed in a small centrifuge tube (1.5 mL) filling it with acetone. The solution was centrifuged at 13000 rpm for 1 min. Nanoparticles precipitated while free molecules stayed in solution. This procedure was repeated at least 5 times producing dye functionalized nanoparticles free of unbound ligands as proven by gel chromatography.

2.2.3.1 Characterization of fluorescently labeled nanoparticles

All the washes were carefully collected and their optical absorption was measured to accurately determine the amount of unreacted dye. By assuming that rest of the dye was uniformly distributed on the nanoparticles, one obtains an average upper limit for the number of dyes per nanoparticle as 14.

## 2.3 Nanoparticle Characterization

All nanoparticles used in the study were characterized as described below.

First, the particles were analyzed with **$^1$H NMR** to establish the absence of unbound ligand molecules through the absence of a sharp peak in their NMR spectrum. A representative spectrum is shown in supplementary figure. 1. Then **FTIR** was used to investigate the packing and order of the ligands on the nanoparticles. A large degree of order consistent with phase separated domains was found for 34-66 OT and 66-34 OT[49]. In the case of the 66-34 br-OT, the spectrum was consistent with a disordered state. Then, the optical spectra were compared to ensure that all of the particles had a similar surface plasmon resonance. Nanoparticles were decomposed using iodine (stock solution 50 mg/mL in methanol) to determine their ligand shell composition. 15 mg of nanoparticle was dissolved in 0.2 mL of water, and 1 mL of the iodine stock solution was added. The mixture was stirred until all the particles had decomposed, as shown by absence of the plasmon peak in the optical spectra of these mixtures. The solvent was removed under vacuum and the residue was redissolved in $CD_3OD$ and $^1$H NMR spectra were used to calculate the ligand shell composition[50]. The metallic core sizes of the nanoparticles were found by dissolving nanoparticles in deionized (DI) water with an approximate optical density of 0.1 and one drop of this solution was placed on top of a carbon coated 200 mesh copper grid (Ladd Research, Vermont, USA) laid over a Kimwipe®. **TEM** images of these substrates were analyzed using ImageJ software and size distributions were obtained by counting at least 200 nanoparticles. Some particles were imaged eight months apart and showed no noticeable change in size distribution. All of the particles

were analyzed using **TGA** to determine the fraction of their weight due to the ligands. The data achieved (when combined with the TEM data) show an approximate ratio of 3 surface gold atoms to 1 thiolated molecule, typical of self-assembled monolayers. Hence all the particles had very similar ligand shell densities. The **solubility** in PBS buffer (pH 7.4) of all nanoparticles was carefully analyzed by first visually determining the saturation concentration (i.e. the appearance of a precipitate). It should be noted that all of the particles studied had a saturation concentration orders of magnitude larger than the one used for cell uptake experiments. To determine the solvation of the particles, their zeta potential was measured with a 0.2 mg/mL nanoparticle solution in PBS buffer (pH 7.4) and serum-free RPMI 1640 medium (Mediatech Inc.) (Supplementary figure. 2).

2.3.1 Characterization of Size Change of Nanoparticles Incubated in Serum-containing Medium

**Gel Filtration Apparatus.** Gel Filtration Chromatography (GFC) was performed using an ÄKTAprime Plus chromatography system from Amersham Biosciences equipped with a Superose 6 10/300 GL column. 16.7mM decanesulfonate and 0.42X PBS was used as the mobile phase with a flow rate of 0.5 mL/min. Nanoparticles before incubation with media were prepared by dissolving 2mg of each nanoparticle in the mobile phase. The incubated nanoparticle samples were obtained by incubation with serum-containing media (RPMI 1640) at a concentration of 0.2 mg/mL for 3 hours at 37 ºC. After the incubation, the samples were concentrated at 3,500 g using a Vivaspin-6 10,000 MWCO spin concentrator to 2mg/mL. GFC was the used to purify the particles. In each run,

200uL of the samples were injected, and 0.2mL fractions were collected. Detection was achieved by measuring the absorption at 280 nm. The 200 μL fractions at the peak position were collected and used for further DLS scan. The column was calibrated using gel filtration protein standards from Bio-Rad (cat. no. 151-1901) ranging in MW from 17 to 670 kDa.

**Dynamic Light Scattering (DLS).** The nanoparticles fractions collected as mentioned above were used for DLS measurements. Light-scattering analysis was performed using a DynaPro Dynamic Light Scatterer. All samples were filtered through a 0.02 μm filter before analysis. Typical count rates were between 70 and 350 kHz. Each autocorrelation function (ACF) was acquired for 10 s, and averaged for 10 min per measurement. A software filter was employed to discard all ACF fits with sum of square errors >30 and with baseline < 0.01. The resulting ACF was fitted using the Dynamics V6 software employing a non-negative least-squares fitting algorithm. Hydrodynamic radii were obtained from a mass-weighted size distribution analysis and reported as the mean of triplicate measurements.

2.3.2 Scanning Tunneling Microscopy (STM) Analysis of Nanoparticles

All STM measurements were performed at room temperature in air. The imaging parameters used were of a set current of 50 pA and a bias voltage comprised between 1 and 1.5 V; imaging speed varied between 0.8 μm/s and 1.8 μm/s. We used platinum-iridium STM tips that were mechanically cut (Digital Instruments). Flame annealed Au(111) on mica substrates were purchased from Molecular Imaging. The sample

preparation methods used in this work are significantly different from our previous studies because strongly hydrophilic particles tend to form very low density layers that are difficult to image due to tip-induced particle movements. Three different sample preparation approaches were found to be somewhat effective for the preparation of layers of these particles. The first approach consisted of preparing nanoparticles in water/ethanol (90:10 vol:vol) mixtures and placing a small drop on a gold substrate preheated to ~ 50 $^{0}$C. This method was most effective for MUS particles. A second approach consisted of placing small water droplets of these nanoparticles (~ 3 mm in diameter) in the center of the gold substrate and rapidly (and gently) enclosing these droplets inside larger toluene (or benzene) droplets. A third approach was to place an ethanol drop in the center of the substrate and then gently add a small microliter drop of an aqueous solution containing the nanoparticles on top of the first drop. All particles were imaged multiple times, using a wide range of imaging parameters and at different imaging speeds. MUS particles showed no features in the ligand shell despite multiple imaging attempts (not even headgroups); 66-34 br OT particles showed (albeit not consistently) some disordered features in their ligand shell; more often they showed no structure at all, in any case ordered structures were never observed. 66-34 OT and 34-66 OT showed the striated pattern that we attribute to 'rippled' particles with a spacing of 1.0 nm ± 0.2 nm and 1.1 nm ± 0.1 nm respectively. Given the challenges involved in imaging hydrophilic nanoparticles, a careful analysis of the images was performed. Images of the latter two particles taken at different scan speeds were evaluated for variations as a function of imaging speed. Additionally, instances in which features on

nanoparticles stayed unaltered across various images were identified in order to further strengthen our conclusions.

**2.4 Characterization of Cellular Uptake of Nanoparticles:**

The nanoparticles after synthesis and characterization (both with and without dye) were dissolved in PBS buffer (pH 7.4) to an approximate concentration of 4 mg/mL. Thereafter, they were passed through a 0.2 μm syringe filter (PTFE membrane) to remove any aggregates. The concentrations of these stock solutions in mg/mL were obtained by optical density measurements.

The mouse dendritic cell (DC) clone, DC2.4, was passaged every 3-4 days in complete RPMI 1640 medium containing 10% fetal bovine serum (FBS obtained from Hyclone), while the mouse embryonic fibroblasts (MEFs obtained from American Type Culture Collection (ATCC)) were cultured in DMEM (Dulbecco's Modified Eagle's Medium with 4.5 g/L of glucose obtained from Mediatech Inc.) containing 15 % FBS.

2.4.1 Confocal Fluorescent Microscopy Studies:

Confocal microscopy was performed on a Zeiss LSM 510 using a 100X oil lens and excitation wavelength set to 633 nm. DC2.4 cells were seeded at 0.5-0.6 X $10^5$ cells per well (cell growth surface area 0.8 $cm^2$) in an 8-well labtek chamber (Nalge Nunc) with 400 μL of RPMI serum-containing medium per chamber. The cells were allowed to grow for 15-17 h, then medium was exchanged with fresh warm serum-free or serum-

containing (10% FBS) medium and nanoparticles were added from a concentrated stock solution in PBS buffer (pH 7.4) at a final concentration of 0.2 mg/mL. Cells were incubated with nanoparticles for 3 h and then washed three times with warm serum-free medium and subsequently imaged on a 37 °C pre-warmed chamber. Control samples without nanoparticle addition were also imaged.

For the confocal studies at 4 °C, the cells were preincubated at 4 °C for 30 minutes before nanoparticle addition. The medium for the nanoparticle incubation and washes and the nanoparticle stock solutions were all preincubated to 4°C before use. Only one to two nanoparticle samples per 8-well labteks were used to obtain images for the studies at 4°C to minimize imaging time. Control samples without nanoparticle addition were also imaged.

The mean fluorescence intensities at 4 ºC were obtained by line scans across the cytosolic regions of cells incubated with or without the nanoparticles through the LSM image browser. At least six different scans were taken and the mean fluorescence intensity over background (arbitrary units) was measured. For each sample, all the scan intensities so obtained were averaged to obtain mean fluorescence intensity.

The confocal studies performed on the MEFs were identical to DCs except that a 40X water immersion lens was used and they were seeded at an initial density of 3 X $10^3$ cells per well in an 8-well labtek chamber with 400 μL of serum-containing DMEM per chamber.

2.4.2 Calcein Uptake/Outleak and Endocytosis Blockage Experiments:

To study the influence of ligand-coated nanoparticles on the uptake of calcein (Invitrogen), 1.4 mg/mL stock of calcein in PBS buffer (pH 7.4) was used. Nanoparticles (with or without dye) at a final concentration of 0.2 mg/mL and calcein at a final concentration of 0.1 mg/mL were added to cells in serum-free RPMI medium. The incubation time was three hours and washing and imaging done similar to other confocal experiments. Calcein was excited at 488 nm, while the dye functionalized nanoparticles were excited at 633 nm as before. Control samples with calcein but without nanoparticles were also studied.

To study the outleak of calcein loaded into the cytosol of cells, calcein-AM (5 μM, purchased from Invitrogen) was preincubated with cells for 45-50 min in serum-containing RPMI medium to load the dye into the cytosol. Cells were then washed three times with warm serum-containing medium. The medium was then replaced with warm serum-free medium and ligand-coated nanoparticles were added to a final concentration of 0.2 mg/mL for 3 h, before washing and imaging as described above.

To observe the nanoparticles entering the cytosol at 37 ºC after blockage of endocytosis, the cells were pretreated with final concentrations of 10 mM and 50 mM of sodium azide (EM Science) and 2-deoxyglucose respectively for 20 min at 37 ºC. Then, calcein (0.2 mg/mL final concentration) was added with or without the nanoparticles (0.2 mg/mL final concentration) and incubated with DCs for another 20 min. Thereafter, the cells were washed and imaged as described above. Control samples without calcein and

nanoparticles, treated under the same conditions were also studied. Z-stack images were taken at a stacking depth size of 1 μm each.

2.4.3 Colony-forming and MTT assays for cell survival/proliferation and viability:

1.3 X $10^5$ DC2.4 cells were seeded per well of a 24 well plate for 17 h with 2 ml of RPMI medium in each well. Before incubation with nanoparticles, the medium was replaced with 1 ml of serum-free medium in each well and the nanoparticles were added from the respective concentrated stock solutions to a final concentration of 0.2 mg/mL in each well. After 3 h of incubation, the cells were washed 3X with serum-free medium, and cells were detached from the plates using trypsin EDTA solution (0.25% trypsin/2.21 mM EDTA purchased from Cellgro). The detached cells were counted and replated in a 96-well plate in triplicate ($10^5$ cells/well) in 200 μL of serum-containing medium. Cells without nanoparticles were seeded in different amounts per well; 500, 2000, 4000, 8000, and 10000 to generate a standard curve. The replated cells were allowed to grow over a period of 24 h and the number of cells present relative to untreated cells was determined using the Cyquant NF cell proliferation assay kit following the manufacturer's instructions (Invitrogen).

For the MTT assay (kit obtained from ATCC), 4 h after replating the cells in a 96-well plate, as described above, 20 μL of MTT reagent was added to each well and further incubated at 37 ºC for 2 h before adding the detergent reagent. The cell density was then determined by the absorbance at 570 nm using a microplate spectrophotometer.

2.4.4 Propidium iodide (PI) staining for cell membrane integrity

1.5 X $10^5$ cells were seeded per well of a 24 well plate for 15 h with 2 mL of RPMI media in each well (with a cell growth surface area of 3.6 $cm^2$). Before incubation with nanoparticles, the media was replaced with 1mL of serum-free media in each well and the nanoparticles were added from the respective concentrated stock solutions to final concentration 0.2 mg/mL in each well. After 3 h incubation, the cells were washed 3X with serum-free media, and were detached from the plates using trypsin/EDTA solution. Then, 1 mL of serum-containing media was added to each well and the cells were centrifuged and resuspended in 1 mL of MACS buffer (PBS, 0.2 % BSA, 0.1 % sodium azide). PI (obtained from Calbiochem, San Diego, CA) was dissolved in MACS buffer upon arrival and 1 μL of PI solution (1 mg/mL) was added to each sample. The samples were kept at 4°C in dark and subsequently analyzed by FACS on FL3 channel. Each nanoparticle concentration was studied in triplicate. Controls were also studied where no nanoparticles were added.

2.4.4 TEM Analysis:

For TEM analysis, cells were grown at an initial seeding amount of 2.5 X $10^6$ cells in a 100 mm cell culture plate (with a cell growth surface area of 59 $cm^2$) for 15 h with 10 ml serum-containing medium in each plate. Thereafter, the medium was replaced by warm serum-free medium and nanoparticles were added from stock solutions to a final concentration of 0.2 mg/mL and incubated for 3 h after which the samples were washed thrice with serum-free medium. The cells were then fixed in 2.5% gluteraldehyde, 3%

paraformaldehyde with 5% sucrose in 0.1M sodium cacodylate buffer (pH 7.4). The cells were pelleted and post-fixed in 1% $OsO_4$ in veronal-acetate buffer. The pellet was stained in block overnight with 0.5% uranyl acetate in veronal-acetate buffer (pH 6.0), then dehydrated and embedded in Spurrs resin.

For each nanoparticle composition, five TEM images were used for counting with at least 6,500 (for serum-free condition) and 6000 (for serum-containing condition) nanoparticles counted per composition. For each image, the cytosolic area (excluding areas such as the nucleus, endosomes and the vesicles) in which one would expect to find free cytosolic nanoparticles was used for counting and the average number of nanoparticles per $\mu m^3$ estimated.

## 3. Supplementary Notes:

### 3.1 References


46. Segall, Y., Quistad, G. B. & Casida, J. E. Cannabinoid CB1 receptor chemical affinity probes: Methods suitable for preparation of isopropyl [11,12-H-3]dodecylfluorophosphonate and [11,12-H-3]dodecanesulfonyl fluoride. *Synth. Commun.* **33**, 2151-2159 (2003).
47. Tien, J., Terfort, A. & Whitesides, G. M. Microfabrication through electrostatic self-assembly. *Langmuir* **13**, 5349-5355 (1997).
48. Templeton, A. C., Cliffel, D. E. & Murray, R. W. Redox and fluorophore functionalization of water-soluble, tiopronin-protected gold clusters. *J. Am. Chem. Soc.* **121**, 7081-7089 (1999).
49. Centrone, A., Hu, Y., Jackson, A. M., Zerbi, G. & Stellacci, F. Phase separation on mixed-monolayer-protected metal nanoparticles: A study by infrared spectroscopy and scanning tunneling microscopy. *Small* **3**, 814-817 (2007).
50. Tognarelli, D. J. *et al.* Covalently networked monolayer-protected nanoparticle films. *Langmuir* **21**, 11119-11127 (2005).